Contrasting H-mode behaviour with fuelling and nitrogen seeding in the all-carbon and metallic versions of JET

G. Maddison [1], C. Giroud [1], M. Beurskens [1], S. Brezinsek [2], P. Devynck [3], T. Eich [4], L. Garzotti [1], S. Jachmich [5], A. Järvinen [6], C. Lowry [7], S. Marsen [4], K. McCormick [4], A. Meigs [1], F. Rimini [1], M. Stamp [1], M. Wischmeier [4] and JET EFDA contributors [†]

JET-EFDA, Culham Science Centre, Abingdon, OX14 3DB, UK.

[1] EURATOM/CCFE Fusion Association, Culham Science Centre, Oxon. OX14 3DB, UK.
[2] IEK-Plasmaphysik, FZ Jülich, Association EURATOM-FZJ, Jülich, Germany.
[3] CEA-Cadarache, Association Euratom-CEA, 13108 St Paul-lez-Durance, France.
[4] Max-Planck-Institut für Plasmaphysik, EURATOM-Association, 85748 Garching, Germany.
[5] Association Euratom-Etat Belge, ERM-KMS, Brussels, Belgium.
[6] Aalto University, Association EURATOM-Tekes, Otakaari 4, 02150 Espoo, Finland.
[7] JET-EFDA/CSU, Culham Science Centre, Abingdon, Oxon. OX14 3DB, UK.

1. Introduction

An all-metal ITER-Like Wall (JET-ILW) [1], consisting of beryllium in the main chamber and tungsten surfaces in the divertor, has now been installed in JET to pursue low retention of fuel species [2] and to explore the impact on next-step-relevant plasmas [3]. Its implementation has offered a unique opportunity to compare behaviour with that in the previous all-Carbon lining (JET-C), notably for high-triangularity Type I H-modes with impurity seeding. This technique is recognised to be necessary for power handling both in ITER and in JET at full performance. Contrasting results are reported for closely-matched deuterium-fuelling plus nitrogen-seeding scans in each JET environment. Attention is focused upon neutral-beam-heated plasmas with total input power 15 - 17 MW at 2.65 T, 2.5 MA, $q_{95} \approx 3.5$, average triangularity $\delta \approx 0.4$, elongation $\kappa \approx 1.7$ and gas inputs spanning ranges $0.75 \leq \Phi_D \leq 3.3$, $0 \leq \Phi_N \leq 4.7$ (10^{22} electrons / s assuming full ionisation). JET-C cases also included 1 - 2 MW of central ion-cyclotron-resonance-frequency heating, so far absent from JET-ILW pulses, with possible consequences for respective core sawtooth and impurity-concentration results.

2. Density, purity and inter-ELM radiation fraction

At high triangularity in the JET-C machine, H-mode density could be raised even slightly above Greenwald level by deuterium puffing without significantly degrading normalised energy confinement [4]. Since such fuelling alone would be insufficient to moderate the exhaust heat load in JET at full power (or ITER), however, extrinsic seeding was also applied to these plasmas. With N injection into the divertor, density then fell again, as shown by the open points in Fig. 1(a). On the other hand, unseeded pulses in JET-ILW began at ≈ 10% lower density for similar fuelling, but then conversely this increased as N was added (filled symbols). These exactly opposite responses reflect corresponding changes in combined particle confinement and fuelling efficiency, which strongly influenced e.g. accompanying inter-ELM total radiated power fraction, as seen in Fig. 1(b). In the JET-C cases, $f_{\rm rad}^{\rm i-E}$ did not change monotonically, but instead actually tended to drop at low N input owing to the loss of density, before rising again for stronger seeding, a variation best seen for higher fuelling. Against this, unseeded plasmas in JET-ILW achieved significantly lower intrinsic impurity content and so higher purity, as anticipated for an all-metal wall, with correspondingly lower

[†] *see appendix of F. Romanelli et al, Proceedings of the 24th IAEA Fusion Energy Conference, October 2012, San Diego, USA.*

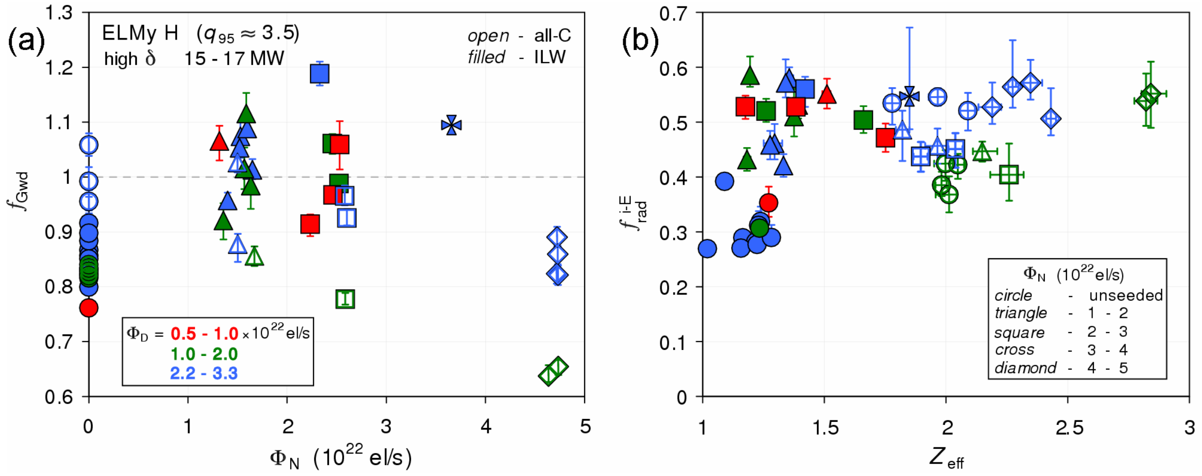

Fig. 1 (a) Normalised density versus N seeding rate. (b) Inter-ELM radiated power fraction versus line-average effective ionic charge (from visible bremsstrahlung). Points colour and symbol coded for D-fuelling and N-seeding rates respectively. Open symbols: JET-C; filled symbols: JET-ILW.

inter-ELM radiation. Mounting N seeding then produced a steady increase in f_{rad}^{i-E} until a level similar to that in the JET-C scans was recovered, though still at Z_{eff} better than or equal to the best JET-C instances, indicating the benefit of replacing dominant C and N impurities with Be and N.

3. Pedestal and energy confinement

Largely owing to the drop in density, N seeding in the JET-C wall resulted in a reduced pedestal and consequent loss of normalised energy confinement, as disclosed in Fig. 2. Here electron edge profiles have been interpolated from high-resolution Thomson scattering data selected during the final third of inter-ELM periods within a 1 - 2 s flat-top window. In contrast, unseeded JET-ILW counterparts at similar fuelling had significantly lower (electron) pedestal pressure and ≈ 30% lower confinement, actually due to a commensurately cooler $T_e^{ped\ i-E}$. Progressively higher N input then induced a recovery in pedestal height and confinement, firstly due to the rise in density, but secondly involving an increase [5] even in $T_e^{ped\ i-E}$ for almost constant pressure. Both JET-ILW and JET-C environments finally realised approximately the same performance for similar fuelling and seeding levels. Best direct proportionality lines separately through each respective dataset reveal the same relationship between pedestal height and confinement was also preserved.

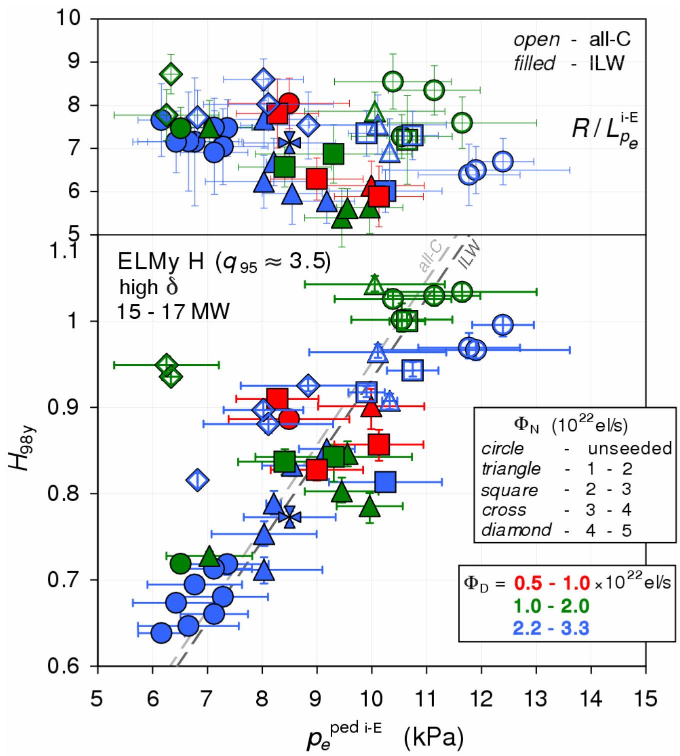

Fig. 2 Normalised energy confinement (bottom) and normalised core electron pressure inverse gradient scale-length between ELMs over $0.3 \le r/a \le 0.8$ (top) versus inter-ELM electron pressure pedestal height. Key as in Fig. 1.

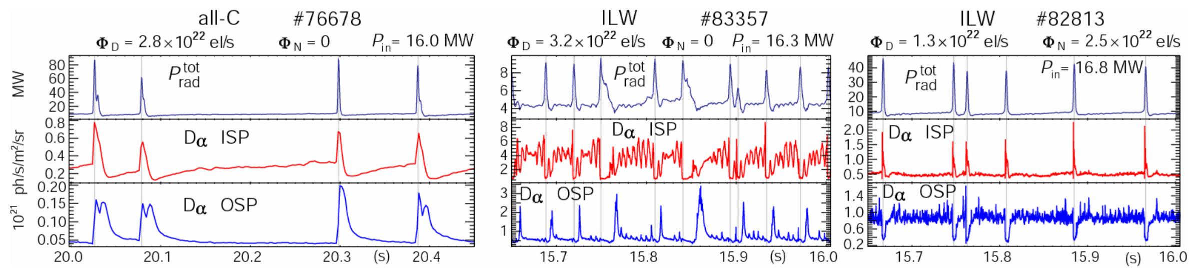

Fig. 3 Total radiated power, Dα emission from the inboard strike-point (ISP) & outboard strike-point (OSP) of the divertor. Examples of (left): unseeded JET-C; (centre): unseeded JET-ILW; (right): N-seeded JET-ILW.

Simultaneously, peaking of core (electron) pressure between ELMs $R|\partial(\ln p_e^{\text{i-E}})/\partial R|$ (top pane, Fig. 2) was almost invariant or even decreasing slightly towards higher confinement, affirming quality of the latter was unequivocally determined by the pedestal. Note JET-ILW cases at lowest fuelling had higher pedestals and confinement, even when unseeded, but on the other hand they were among the least steady plasmas, as outlined below.

4. Divertor recycling, power balance and impurity sources

Recycling imposes a fundamental boundary condition on tokamak plasmas and would be expected to be particularly affected by the change from all-C to all-metal walls. Responses during Type I ELMing in the JET-C machine are typified in Fig. 3 (left). Within measurement uncertainties, (either without or with N seeding,) each ELM crash induced near-coincident spikes in total radiation and recycling at the divertor inboard and outboard strike-points. In JET-ILW, however, unseeded average Dα emission was roughly 10× brighter at both strike-points than in the JET-C situation for similar fuelling and power. Moreover, inboard - outboard asymmetric effects emerged at ELMs (ISP fall, OSP rise), as well as in spontaneous divertor oscillations [6], here at ~ 200 Hz, between them. These latter fluctuations tended to be suppressed when N was added, while the in - out asymmetry at ELMs persisted but reversed at higher seeding levels (ISP rise, OSP fall). Hence a higher recycling regime and radically different dynamics / inter-ELM detachment followed from the change to W divertor surfaces.

The primary aim of impurity seeding is to reduce heat loads on the divertor targets by dispersing power as radiation. The balance firstly between ELMs has been estimated by averaging quantities over intervals 50 - 90% of the way between neighbouring peaks during 1 - 2 s flat-top windows. Fractional power load on the whole toroidal outboard target has been derived from fast IR thermography for JET-C cases and, lacking this generally, from embedded Langmuir probes with a sheath transmission factor $\gamma = 8$ in JET-ILW. The latter data are restricted to pulses with best-defined probe profiles, checked in three instances available to agree well with thermography. Results are plotted against inter-ELM exhaust fraction in Fig. 4, where it becomes clear that in JET-ILW, outboard target load declined in proportion to the total radiative cooling ($P_{\text{rad}}^{\text{i-E}}$) plus ELM recurrence ($\partial W^{\text{i-E}}/\partial t$) effects of N injection. Discounting two outlying pulses which reverted to Type III regime, a similar outcome prevailed in the JET-C scans. By averaging ELM energy amplitude divided by the preceding inter-ELM period ($\Delta W^{\text{ELM}}/\Delta t^{\text{i-E}}$) over the same flat-top windows, an approximation of overall power efflux (i.e. ejected onto all surfaces) from these fluctuations can also be extracted; recall this differs from peak power load transiently achieved in each ELM burst. A priori a simple relation to inter-ELM exhaust would not necessarily be expected and such a departure seems to have been borne out for the JET-C plasmas. Surprisingly, though, total ELM power fraction in JET-ILW again decreased roughly in proportion with the impact of N, adding a significant bonus to its use.

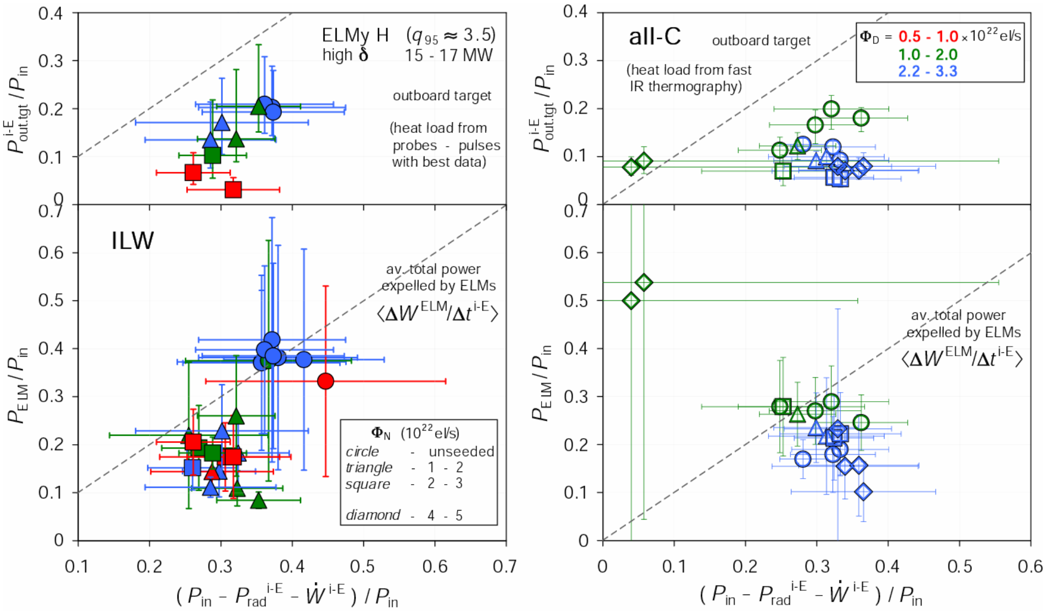

Fig. 4 Power fractions (top) landing on the outboard target between ELMs and (bottom) ejected by ELMs versus inter-ELM exhaust fraction. (Left): JET-ILW (top: only pulses with target probes best defining heat load); (right): JET-C. Key as in Fig. 1.

ELM loads also tend to dominate intrinsic impurity sources [7], particularly of W in the JET-ILW divertor and especially in the presence of heavier, higher-charge N ions. This erosion led to gradual contamination of JET-ILW seeded plasmas which was only weakly ameliorated by higher-frequency ELMs and produced unsteadiness which remains the principal limitation of JET-ILW operations so far. However their lack of central ICRH, mentioned above, may have exacerbated core impurity build-up compared to JET-C cases incorporating such local heating.

5. Conclusion

Replacing the former all-C wall in JET with all-metal surfaces has markedly changed the plasma boundary conditions and intrinsic impurity characteristics. Pedestal, confinement and ELM behaviour have all been found to be strongly affected. However, seeding with N has not only succeeded in reducing divertor heat loads, between and even for ELMs, but also beneficially recovered much of the all-C performance by helping to raise plasma density and, for the first time in JET, electron pedestal temperature. Attention in next experiments will be on controlling W contamination, improving stationarity and testing noble gases further to extend development of a full-power, long-pulse H-mode scenario.

This work, part-funded by the European Communities under the contract of Association between EURATOM/CCFE and by the RCUK Energy Programme [grant number EP/I501045], was supported by EURATOM and carried out within the framework of the European Fusion Development Agreement. The views and opinions expressed herein do not necessarily reflect those of the European Commission.

References

[1] G. F. Matthews *et al* Physica Scripta **T128** (2007) 137
[2] S. Brezinsek *et al* 24th IAEA Fusion Energy Conf. (San Diego, CA, USA, Oct. 2012) EX/4-1 *
[3] E. Joffrin *et al* *ibid.* EX/1-1 *
[4] A. Loarte *et al* Plasma Physics and Controlled Fusion **44** (2002) 1815
[5] C. Giroud *et al* 24th IAEA Fusion Energy Conf. (San Diego, CA, USA, Oct. 2012) EX/P5-30 *
[6] S. I. Krasheninnikov *et al* Nuclear Fusion **27** (1987) 1805.
[7] G. J. van Rooij *et al* 20th Int. Conf. Plasma Surface Interactions (Aachen, Germany, May 2012) I3, *in press*, Journal of Nuclear Materials (2013)
* *submitted to* Nuclear Fusion